A multi-group extended linear discontinuous method for fixed-source discrete ordinates problems in slab geometry

Iram B. Rivas-Ortiz

Instituto Superior de Tecnologías y Ciencias Aplicadas,
Universidad de la Habana,
Quinta de los Molinos, Ave. Salvador Allende 1100,
e/Infanta y Rancho Boyeros, Vedado, La Habana, Cuba
Email: ibrivas@instec.cu

Dany S. Dominguez*

Pós-graduação em Modelagem Computacional,
Universidade Estadual de Santa Cruz,
Rodovia Jorge Amado, km 16, Salobrinho,
45662-900 Ilhéus, BA, Brazil
Email: dsdominguez@gmail.com
*Corresponding author

Carlos R. García Hernández

Instituto Superior de Tecnologías y Ciencias Aplicadas,
Universidad de la Habana,
Quinta de los Molinos, Ave. Salvador Allende 1100,
e/ Infanta y Rancho Boyeros, Vedado, La Habana, Cuba
Email: cgh@instec.cu

Susana M. Iglesias

Pós-graduação em Modelagem Computacional,
Universidade Estadual de Santa Cruz,
Rodovia Jorge Amado, km 16, Salobrinho,
45662-900 Ilhéus, BA, Brazil
Email: smiglesias@uesc.br

Abstract: At present, neutron density calculation in non-multiplying media is relevant in many areas of engineering and science. In this paper, we propose the Extended Linear Discontinuous (ELD) method in multi-group discrete ordinates formulation, originally formulated for one-energy group fixed-source problems with isotropic scattering source in slab geometry. The proposed auxiliary equations are uncoupled on angular directions and combine the linear discontinuous approximation of the finite element method and the quasi-analytical general solution of the spectral nodal method. Thus, we can implement an efficient and simple algorithm using the conventional source iteration scheme for the sweeping equations. Numerical results for benchmark

problems are presented to illustrate the accuracy and computational performance of the ELD method. The work shows that the main advantages of the proposed method are that the numerical scheme is stable for coarse-meshes, and its numerical results are more accurate than those generated by the Diamond Difference (DD) and Linear Discontinuous (LD) methods.

Keywords: multi-group transport problems; discrete ordinate formulation; fixed-source problems; linear discontinuous.

Reference to this paper should be made as follows: Rivas-Ortiz, I.B., Dominguez, D.S., Hernández, C.R.G. and Iglesias, S.M. (2019) 'A multi-group extended linear discontinuous method for fixed-source discrete ordinates problems in slab geometry', *Int. J. Nuclear Energy Science and Technology*, Vol. 13, No. 1, pp.70–86.

Biographical notes: Iram B. Rivas-Ortiz completed his Bachelor and Master degrees in Nuclear Engineering from Instituto Superior de Tecnologías y Ciencias Aplicadas (InSTEC). His main research interests are numerical methods for nuclear engineering problems. Currently, he is a PhD Student in Computing Modelling at Universidade do Estado do Rio de Janeiro.

Dany S. Dominguez graduated in 1998 from Highest Institute in Nuclear Science and Technologies, Havana, Cuba, in nuclear engineering. He received the DSc (PhD) degree from Rio de Janeiro State University in Computing Modelling with emphasis on transport particles (2006). His main research interests are numerical methods for computing modelling nuclear reactors and transport radioactivity problems, applied computer and numerical analysis. Currently, he is a Full Professor of Santa Cruz State University in Bahia, Brazil.

Carlos R. García Hernández is a Professor in Instituto Superior de Tecnologías y Ciencias Aplicadas (InSTEC). He received his PhD and BSc degrees in Nuclear Engineering in 1997 and 1981, respectively from Instituto Superior Jose Antonio Echeverria (CUJAE). He has researched in nuclear reactors physics since more than 30 years. He has published more than 30 papers in international journals.

Susana M. Iglesias obtained her Computer Science degree from the Havana University, Cuba, in 1998. She received her Computer Modelling PhD from the Rio de Janeiro State University, in 2008. She is a Full Professor in the Science and Technology Department of the Santa Cruz State University, Ilheus, Brazil. Her research interests include applied computer, numerical methods and applied nuclear techniques.

1 Introduction

The transport theory emerges as a result of the need to describe, using a mathematical model, different physical phenomena in the fields of gas dynamics, radioactive transfer, plasma theory, and sound propagation. On the other hand, the neutron population in both multiplying and non-multiplying media, is relevant in several areas such as nuclear reactor theory, materials science and radiological protection. This work approaches the neutron density calculations in non-multiplying media. In these cases, the mathematical model used is the neutron transport equation.

The deterministic methods' use to solve neutron transport problems is widely reported in the scientific literature (Alcouffe et al., 1979; Larsen, 1986; Barros and Larsen, 1990; Barros et al., 1998; Filho et al., 2002; Dominguez and Barros, 2007; Barros et al., 2010; Menezes et al., 2014; Silva et al., 2015). In many instances, it is common to use the multi-group discrete ordinate formulation (S_N) of neutron transport equation as the mathematical model (Lewis and Miller, 1984). The computational power demanded solving the S_N transport equations is technically expensive since it involves high CPU times and large memory storage. For this reason, the research in this field devotes much effort to obtain numerical results with good accuracy for coarse spatial discretisation.

In the last three decades, much attention has been given to spectral nodal methods. The essence of these methods, reported by Larsen (1986), is to use the "spectrum" of the S_N transport equations to estimate the average angular flux in each spatial discretisation cell called "node". The first spectral nodal method, described in Barros and Larsen (1990) called spectral Green's function method (SGF) was developed to solve problems with fixed-source, one-dimensional Cartesian geometry, and one-energy group. From this point, various authors extended the SGF methods for several groups, anisotropic source term, different geometries and transport equation formulations, both for fixed-source like (Barros and Larsen, 1991; Barros and Larsen, 1992; Anli and Gungor, 1996; Barros, 1997; Barros et al., 1998; Mello and Barros, 2002; Dominguez and Barros, 2007; Barros et al., 2010; Menezes et al., 2014) as well as for eigenvalue problems (Abreu et al., 1996; Barros et al., 1999; Filho et al., 2002; Barros et al., 2003; Silva et al., 2015). The main advantages of SGF methods are their high accuracy and weak spatial dependence. However, they present a high computational cost and complex numerical algorithms associated with the one-Node Block Inversion (NBI) iterative schemes (Barros and Larsen, 1991; Dominguez and Barros, 2007). The SGF-methods must use NBI-schemes because the auxiliary equations are coupled in angular directions.

Recently, several publications focus on the development of new numerical approaches that offer an acceptable compromise between accuracy and computational cost (Dominguez et al., 2010; Rocha et al., 2016; Dominguez et al., 2018). Rivas-Ortiz et al. (2019) proposed the Extended Linear Discontinuous (ELD) method in discrete ordinates formulation for the resolution of one-energy group fixed-source problems. This method is simples and characterised by a weak spatial dependence on the generated numerical results. The ELD method's advantages are based on the use of uncoupled auxiliary equations, allowing to implement a conventional source iteration sweep scheme.

In this paper, we propose the ELD method in multi-group discrete ordinates approach for the solution of fixed-source problems with isotropic scattering in slab geometry. Furthermore, we verify its accuracy and performance by solving benchmarks problems. Firstly, the mathematical formulation is developed and then, we describe the iterative sweeping scheme used. Finally, two benchmark problems are solved using the proposed method. The numerical results are compared with the solutions generated by the Diamond Difference (DD) (Lewis and Miller, 1984), Linear Discontinuous (LD) (Alcouffe et al., 1979) and SGF (Barros and Larsen, 1991) methods.

2 Mathematical formulation for multi-group ELD method

We consider a generic slab geometry fixed source transport problem with prescribed boundary conditions in a domain of length *X*. For neutron density calculations the multi-group discrete ordinates formulation of neutron transport equation is used as a mathematical model

$$\mu_m \frac{d}{dx}\psi_{m,g}(x)+\sigma_{t,g}(x)\psi_{m,g}(x)=\sum_{g'=1}^{G}\frac{\sigma_{s,g',g}^{(0)}(x)}{2}\sum_{n=1}^{N}\psi_{n,g'}(x)\omega_n+Q_g(x) \tag{1}$$

$$\psi_{m,g}(0)=L_{m,g},\ \mu_m>0,\quad m=1,2,\ldots,\frac{N}{2}$$

$$\psi_{m,g}(\mathrm{X})=R_{m,g},\ \mu_m<0,\quad m=\frac{N}{2}+1,\frac{N}{2}+2,\ldots,N$$

with $0\le x\le X$, $m=1,\ldots,N$ and $g=1,\ldots,G$. In equation (1) $\psi_{m,g}(x)$ is the angular flux per ordinate direction m and energy group g. $\sigma_{t,g}(x)$, $\sigma_{s,g',g}^{(0)}(x)$ and $Q_g(x)$ represent the total macroscopic cross-section, zero-order component of the differential scattering macroscopic cross-section and fixed-source, respectively. μ_m constitutes the discrete ordinate direction and, ω_m the weights of the Gauss-Legendre quadrature. $L_{m,g}$ and $R_{m,g}$ are prescribed functions. N is the order of the quadrature and G is the energy groups number.

In order to solve the system of $G\times N$ ordinary differential equations above, equation (1), we discretised our spatial domain in a number I of cells (see Figure 1). The size h_i of each cell is chosen so that the macroscopic cross-sections $\sigma_{t,g}(x)$, $\sigma_{s,g',g}^{(0)}(x)$ and fixed-source $Q_g(x)$ are constant piecewise functions inside the spatial cells.

Figure 1 Spatial domain divided into *I* cells

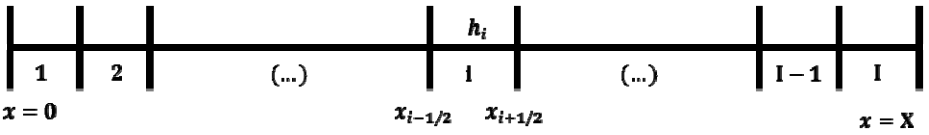

At this point the S_N spatial balance equations in each cell $(i=1,\ldots,I)$ are obtained by applying the operator

$$\frac{2l+1}{h_i}\int_{x_{i-1/2}}^{x_{i+1/2}}P_l\left[\frac{2(x-x_i)}{h_i}\right]\cdot dx,\quad \text{for}\quad x_i=\frac{x_{i-1/2}+x_{i+1/2}}{2} \tag{2}$$

in the S_N transport equations. P_l represents the l-degree Legendre polynomial. Considering $l = 0$, we get the zero-order balance equations

$$\frac{\psi_{m,g,i+1/2} - \psi_{m,g,i-1/2}}{\alpha^x_{m,g,i}} + \overline{\psi}_{m,g,i} = \overline{S}_{g,i} + \frac{Q_{g,i}}{2\sigma_{t,g,i}} \tag{3}$$

and for $l = 1$ the first-order balance equations

$$\frac{3\left[\psi_{m,g,i+1/2} + \psi_{m,g,i-1/2} - 2\overline{\psi}_{m,g,i}\right]}{\alpha^x_{m,g,i}} + \hat{\psi}_{m,g,i} = \hat{S}_{g,i} \tag{4}$$

where the zero and first-order moments of angular flux have the form

$$\overline{\psi}_{m,g,i} = \frac{1}{h_i}\int_{x_{i-1/2}}^{x_{i+1/2}} \psi_{m,g}(x)\,dx \tag{5}$$

$$\hat{\psi}_{m,g,i} = \frac{6}{h_i^2}\int_{x_{i-1/2}}^{x_{i+1/2}} (x - x_i)\,\psi_{m,g}(x)\,dx \tag{6}$$

In addition, the scattering source terms of zero and first-order are defined as

$$\overline{S}_{g,i} = \frac{1}{2}\sum_{g'=1}^{G} c^{(0)}_{g',g,i} \sum_{n=1}^{N} \overline{\psi}_{n,g',i} w_n \tag{7}$$

$$\hat{S}_{g,i} = \frac{1}{2}\sum_{g'=1}^{G} c^{(0)}_{g',g,i} \sum_{n=1}^{N} \hat{\psi}_{n,g',i} w_n \tag{8}$$

and the auxiliary constants

$$c^{(0)}_{g',g,i} = \frac{\sigma^{(0)}_{s,g',g,i}}{\sigma_{t,g,i}} \tag{9}$$

$$\alpha^x_{m,g,i} = \frac{h_i \sigma_{t,g,i}}{\mu_m} \tag{10}$$

The set of zero and first-order spatial balance equations, equations (3) and (4), with the corresponding boundary conditions form an undetermined linear algebraic system with an infinite number of solutions. Therefore, it is necessary to specify some auxiliary equations to transform the system into a fully determined system with a unique solution.

The ELD method auxiliary equations for several energy groups use the linear discontinuous approximation of the finite element methods (Hill, 1975; Rocha et al., 2016) introducing two additional spectral parameters. These parameters are calculated using the general quasi-analytical solution of the S_N one-dimensional multi-group spectral nodal method (Barros and Larsen, 1991). The auxiliary equations of the proposed ELD method in each spatial cell have the form

$$\psi_{m,g}(x) = A_{k,i}\overline{\psi}_{m,g,i} + \frac{2(x - x_i)}{h_i} B_{k,i}\hat{\psi}_{m,g,i} + (1 - A_{k,i})\psi^p_{m,g,i}, \quad x_{i-1/2} \le x \le x_{i+1/2} \tag{11}$$

where $A_{k,i}$ and $B_{k,i}$ constitute the spectral parameters. $\psi^{p}_{m,g,i}$ is a constant function and represents the particular solution of equation (1) in each cell. From the spectral analysis of equation (1), reported by Barros and Larsen (1991) for several energy groups, the general quasi-analytical solution has the form

$$\psi_{m,g}(x) = \psi^{p}_{m,g} + \sum_{k=1}^{GN} \alpha_k a_{m,g}(\vartheta_k) e^{x/\vartheta_k} \tag{12}$$

where $a_{m,g}(\vartheta_k)$ represents the problem's eigenvectors associated with the eigenvalue ϑ_k, and α_k are arbitrary constants. Then, replacing the equation (12) in equations (5) and (6), we obtain the quasi-analytical expressions of the zero and first-order moment of angular flux, respectively

$$\bar{\psi}_{m,g,i} = \psi^{p}_{m,g,i} + \sum_{k=1}^{GN} \alpha_k \frac{2\vartheta_k a_{m,g}(\vartheta_k)}{h_i} senh\left(\frac{h_i}{2\vartheta_k}\right) e^{\frac{x_i}{\vartheta_k}} \tag{13}$$

$$\hat{\psi}_{m,g,i} = \sum_{k=1}^{GN} \alpha_k \frac{6\vartheta_k a_{m,g}(\vartheta_k)}{h_i} \left[\cosh\left(\frac{h_i}{2\vartheta_k}\right) - \frac{2\vartheta_k}{h_i} senh\left(\frac{h_i}{2\vartheta_k}\right)\right] e^{\frac{x_i}{\vartheta_k}} \tag{14}$$

Once obtained the expressions of each term that appear in the equation (11), the auxiliary equations have the form

$$\begin{aligned} \sum_{k=1}^{GN} \alpha_k a_{m,g}(\vartheta_k) e^{x/\vartheta_k} = {} & A_{k,i} \sum_{k=1}^{GN} \alpha_k \frac{2\vartheta_k a_{m,g}(\vartheta_k)}{h_i} senh\left(\frac{h_i}{2\vartheta_k}\right) e^{\frac{x_i}{\vartheta_k}} \\ & + B_{k,i} \frac{2(x-x_i)}{h_i} \sum_{k=1}^{GN} \alpha_k \frac{6\vartheta_k a_{m.g}(\vartheta_k)}{h_i} \left[\cosh\left(\frac{h_i}{2\vartheta_k}\right) - \frac{2\vartheta_k}{h_i} senh\left(\frac{h_i}{2\vartheta_k}\right)\right] e^{\frac{x_i}{\vartheta_k}} \end{aligned} \tag{15}$$

Matching term by term in equation (15) we get

$$e^{x/\vartheta_k} = e^{\frac{x_i}{\vartheta_k}} \left\{ A_{k,i} \frac{2\vartheta_k}{h_i} senh\left(\frac{h_i}{2\vartheta_k}\right) + B_{k,i} \frac{2(x-x_i)}{h_i} \frac{6\vartheta_k}{h_i} \left[\cosh\left(\frac{h_i}{2\vartheta_k}\right) - \frac{2\vartheta_k}{h_i} senh\left(\frac{h_i}{2\vartheta_k}\right)\right] \right\} \tag{16}$$

The equation (16) is a general expression that we will use for the calculation of the spectral parameters. This expression must be satisfied at each spatial cell-edges. Evaluating the equation (16) for the left-edge ($x = x_{i-1/2}$) and the right-edge ($x = x_{i+1/2}$) and after several manipulations, a system of two linear algebraic equations is achieved

$$e^{-h_i/2\vartheta_k} = A_{k,i} \frac{2\vartheta_k}{h_i} senh\left(\frac{h_i}{2\vartheta_k}\right) - B_{k,i} \frac{6\vartheta_k}{h_i} \left[\cosh\left(\frac{h_i}{2\vartheta_k}\right) - \frac{2\vartheta_k}{h_i} senh\left(\frac{h_i}{2\vartheta_k}\right)\right] \tag{17}$$

$$e^{h_i/2\vartheta_k} = A_{k,i} \frac{2\vartheta_k}{h_i} senh\left(\frac{h_i}{2\vartheta_k}\right) + B_{k,i} \frac{6\vartheta_k}{h_i} \left[\cosh\left(\frac{h_i}{2\vartheta_k}\right) - \frac{2\vartheta_k}{h_i} senh\left(\frac{h_i}{2\vartheta_k}\right)\right] \tag{18}$$

whose solution is determined by the expressions

$$A_{k,i} = \frac{h_i}{2\vartheta_k} \coth\left(\frac{h_i}{2\vartheta_k}\right) \tag{19}$$

$$B_{k,i} = \frac{h_i}{6\vartheta_k\left[\coth\left(\frac{h_i}{2\vartheta_k}\right) - \frac{2\vartheta_k}{h_i}\right]} \tag{20}$$

As it can be seen in equations (19) and (20), $A_{k,i}$ and $B_{k,i}$ parameters depend on the ϑ_k eigenvalues. The main idea that supports the multi-group ELD method is to preserve the greater magnitude eigenvalue in the numerical scheme. This choice is consistent with the Larsen (1986) work, where the greater eigenvalue is preserved to construct the Extended Diamond numerical scheme. In our numerical strategy the quasi-analytical solution equation (12), is a sum of exponential functions. The associated function to the greater eigenvalue is dominant and, consequently, the more significant term in the quasi-analytical solution. When we preserve this eigenvalue, the dominant exponential term behaviour is reproduced by the ELD numerical scheme. Therefore, we set $k=1$, referred to the maximum eigenvalue, in the equations (19) and (20), and substituting the spectral parameters in equation (11) getting

$$\psi_{m,g}(x) = \frac{h_i}{2\vartheta_1}\coth\left(\frac{h_i}{2\vartheta_1}\right)\bar{\psi}_{m,g,i} + \frac{2(x-x_i)}{6\vartheta_1\left[\coth\left(\frac{h_i}{2\vartheta_1}\right) - \frac{2\vartheta_1}{h_i}\right]}\hat{\psi}_{m,g,i} + \left[1 - \frac{h_i}{2\vartheta_1}\coth\left(\frac{h_i}{2\vartheta_1}\right)\right]\psi^p_{m,g,i} \tag{21}$$

The decision to preserve the maximum eigenvalue guarantees that the others eigenvalues ϑ_k $(k=2\ldots N)$, do not tend to be infinite or are complex, for any value of h_i. This approximation partially preserves the multi-group S_N slab geometry problem kernel. Specifically, two eigenvalues (the greater and the corresponding conjugate) in the kernel of $N\times G$ size are preserved. For that reason, this approximation is rougher when compare with the SGF approach where the S_N kernel is fully preserved. Therefore, the proposed method has a weak spatial grid dependence on the numerical results generation.

3 Iterative sweeping scheme

The procedure used to solve the S_N transport equations in multi-group discrete ordinates approximation is supported by an iterative scheme on the scattering source terms, called Source Iteration (SI) (Lewis and Miller, 1984). The SI schemes are simpler when compared with NBI schemes.

The SI sweep scheme runs through all the cells of the spatial domain, first for the left-to-right directions $(\mu_m > 0)$ in which the neutrons travel, and then for the right-to-left directions $(\mu_m < 0)$ (see Figure 2). In each cell, the exiting angular fluxes are estimated by the following steps for each angular direction and energy group:

I The scattering source terms $\left(\overline{S}_{g,i}\,,\hat{S}_{g,i}\right)$ and the incoming angular flux $\left(\psi_{m,g,i\mp1/2}\right)$ are used to obtain the zero and first-order moment of angular flux $\left(\overline{\psi}_{m,g,i}\right.$ and $\left.\hat{\psi}_{m,g,i}\right)$.

II Then, the calculated angular fluxes moments are used to obtain the exiting cell-edge angular flux $\left(\psi_{m,g,i\pm1/2}\right)$ using the auxiliary equations.

III Finally, after finishing the left-to-right and right-to-left sweeps, the stop criterion is verified and the iterative process finishes, or if not, the scattering source terms are updated for the next iteration.

Figure 2 Iterative sweeping process used by the ELD method for the left-to-right $\left(\mu_m>0\right)$ and right-to-left $\left(\mu_m<0\right)$ directions in which the neutrons travel

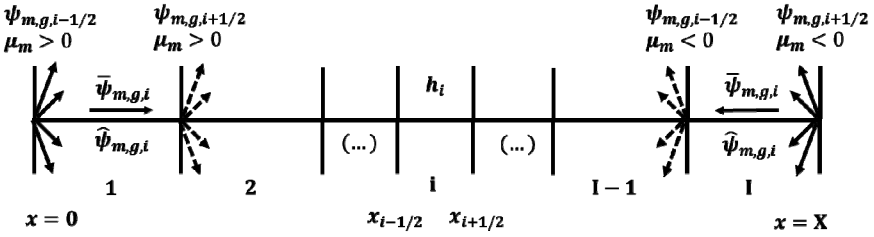

In step (I) of the algorithm, the zero and first-order moment of angular flux are estimated by the expressions

$$\overline{\psi}_{m,g,i}=\frac{\pm\left|\alpha^{x}_{m,g,i}\right|B_i\hat{S}_{g,i}-\left(6B_i+\left|\alpha^{x}_{m,g,i}\right|\right)\psi_{m,g,i\mp1/2}+\left|\alpha^{x}_{m,g,i}\right|\left(1-A_i\right)\psi^{p}_{m,g,i}}{B_i\left(3A_i-6\right)-\left(3B_i+\left|\alpha^{x}_{m,g,i}\right|\right)\left(A_i+\left|\alpha^{x}_{m,g,i}\right|\right)}$$
$$-\frac{\left|\alpha^{x}_{m,g,i}\right|\left(3B_i+\left|\alpha^{x}_{m,g,i}\right|\right)\left(\overline{S}_{g,i}+Q_{g,i}/2\sigma_{t,g,i}\right)}{B_i\left(3A_i-6\right)-\left(3B_i+\left|\alpha^{x}_{m,g,i}\right|\right)\left(A_i+\left|\alpha^{x}_{m,g,i}\right|\right)} \tag{22}$$

$$\overline{\psi}_{m,g,i}=\frac{-\left|\alpha^{x}_{m,g,i}\right|\left(A_i+\left|\alpha^{x}_{m,g,i}\right|\right)\hat{S}_{g,i}\pm\left(6A_i-6+3\left|\alpha^{x}_{m,g,i}\right|\right)\psi_{m,g,i\mp1/2}\pm\left(1-A_i\right)\left(6+3\left|\alpha^{x}_{m,g,i}\right|\right)\psi^{p}_{m,g,i}}{B_i\left(3A_i-6\right)-\left(3B_i+\left|\alpha^{x}_{m,g,i}\right|\right)\left(A_i+\left|\alpha^{x}_{m,g,i}\right|\right)}$$
$$\pm\frac{\left|\alpha^{x}_{m,g,i}\right|\left(3A_i-6\right)\left(\overline{S}_{g,i}+Q_{g,i}/2\sigma_{t,g,i}\right)}{B_i\left(3A_i-6\right)-\left(3B_i+\left|\alpha^{x}_{m,g,i}\right|\right)\left(A_i+\left|\alpha^{x}_{m,g,i}\right|\right)} \tag{23}$$

which are obtained solving the linear algebraic system conformed for the zero and first-order spatial balance equations (equations (3) and (4), respectively), together with the auxiliary equations (see equation (21)). Here, the spectral parameters A_i and B_i corresponds to $A_{1,i}$ and $B_{1,i}$ evaluating $k=1$ in equations (19) and (20).

The calculation of the exiting cell-edge angular flux in each cell, referred in the step (II), is made using the auxiliary equations in the form

$$\psi_{m,g,i\pm1/2} = A_i\overline{\psi}_{m,g,i} \pm B_i\hat{\psi}_{m,g,i} + \left(1 - A_i\right)\psi^{p}_{m,g,i} \tag{24}$$

In the equations (22), (23) and (24) is considered the upper signs for the sweep from to the left-to-right $\left(\mu_m > 0\right)$ and the lower signs for the sweep from the right-to-left $\left(\mu_m < 0\right)$.

Finally, in step (III) the scattering source terms are initialised to zero and then, updated in each iteration using equations (7) and (8).

The iterative SI swept scheme is simpler and uses a smaller number of computational operations per iteration than the NBI scheme. Nevertheless, the NBI iterative scheme must be used on the SGF method. Therefore, a lower computational cost and simpler implementation is expected for the ELD method if compared with the SGF method.

4 Results and discussion

In this section, two benchmark problems are solved by the ELD method. The accuracy is evaluated using the numerical results relative deviation and the computational performance is estimated by the CPU times. The numerical solutions are compared with the obtained by the DD, LD and SGF methods.

Our first model problem with two-energy groups, was proposed by Barros and Larsen (1991) and involves a 100 cm length heterogeneous slab divided into four regions. The material regions constants and geometry details are shown in Figure 3. On the domain left boundary we have reflexive boundary conditions, and in the right one, vacuum boundary conditions.

Figure 3 Two-energy group heterogeneous benchmark problem

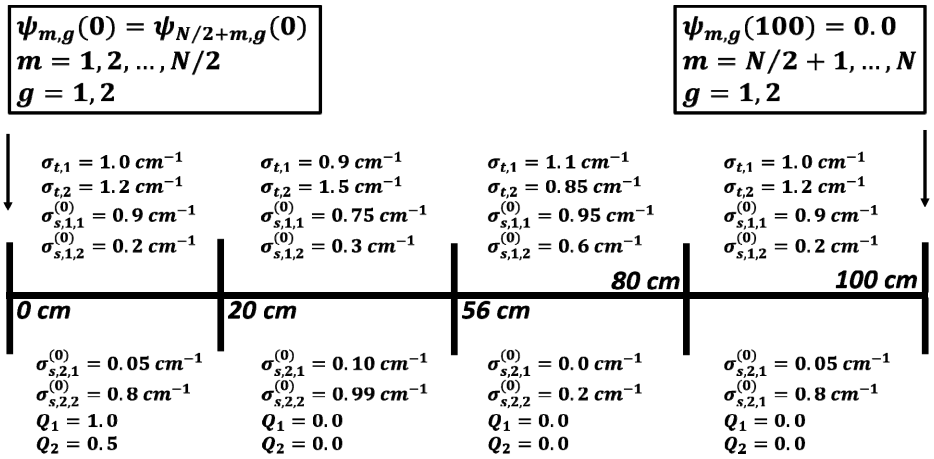

Tables 1 and 2, record the scalar flux at the x = 20, 56 and 80 cm positions, the group relative deviation $\left(\delta_g\right)$ and the CPU time for the generated numerical results using ELD,

DD, LD, and SGF methods. Table 1 has the results for S_2 quadrature order and Table 2 for S_{16}. The group relative deviation represents the maximum relative deviation per group and is calculated, according to (Alcouffe et al., 1979) as

$$\delta_g = \max_{i \in I} \frac{\left| \phi_{g,i+1/2} - \phi^{ref.}_{g,i+1/2} \right|}{\left| \phi^{ref.}_{g,i+1/2} \right|} \tag{25}$$

In the calculation of the group relative deviation, we consider as reference solution, the numerical results generated by the SGF method with the fine-mesh (160×288×192×160 cells). This reference solution can be obtained also, using the DD method with finer mesh (5000×9000×6000×5000 cells), but this is computationally expensive. We used 1E-8, as the iterative process stopping criteria. In Figure 4, we show the two-group neutron distribution generated by the DD, LD and ELD methods in coarse mesh and also the SGF reference solution.

Tables 1 and 2 show that the numerical results generated by the ELD, DD and LD methods come nearer to the reference solution when the mesh become finer. The multi-group ELD method has a weak spatial dependence for the coarse mesh (5×9×6×5 cells) but is not spatial truncation error free like in one-energy group problems and S_2 quadrature (Rivas-Ortiz et al., 2018). This is a consequence of preserving only two eigenvalues, while the $(G \times N - 2)$ remaining, are not preserved. However, the proposed method is more accurate if compared with the DD and LD methods for the coarse mesh studied and the non-conserved eigenvalues play a weak role in the numerical result accuracy.

Table 1 Numerical results for the two-group heterogeneous benchmark problem with S_2 quadrature

Method	*Mesh*	*x = 20*	*x = 56*	*x = 80*	δ_g	*CPU (s)*
ELD	32M[a]	3.3024e+00[b] 2.1363e+00[c]	1.0104e-07 7.2529e-08	5.7441e-15 6.9735e-15	3.2282e-06 2.0844e-05	1.0197e+01
	M	3.3025e+00 2.1295e+00	1.0119e-07 7.2974e-08	5.7470e-15 6.4683e-15	1.7803e-02 3.7942e-01	3.4260e-01
DD	32M	3.3024e+00 2.1363e+00	1.0053e-07 7.2158e-08	5.6528e-15 6.8626e-15	1.8395e-02 1.8395e-02	8.4193e+00
	M	3.3024e+00 2.1363e+00	–1.4606e-05 3.5632e-05	3.8351e-08 5.0455e-07	2.5141e+09 3.3849e+10	3.4260e-01
LD	32M	3.3024e+00 2.1363e+00	1.0103e-07 7.2522e-08	5.7423e-15 6.9712e-15	3.7009e-04 3.7050e-04	1.0552e+01
	M	3.3085e+00 2.1130e+00	1.2608e-08 8.8144e-09	–2.4934e-16 –3.0542e-15	1.1045e+00 1.4380e+00	3.6805e-01
SGF	32M	3.3024e+00 2.1363e+00	1.0104e-07 7.2529e-08	5.7441e-15 6.9735e-15	Ref.	1.6675e+01
	M	3.3024e+00 2.1363e+00	1.0104e-07 7.2529e-08	5.7441e-15 6.9735e-15	2.1625e-08 2.3004e-08	1.8337e-01

Note: [a]M = 5×9×6×5 cells,
[b]Scalar flux (Group 1) = 3.3024 n.cm^2/s,
[c]Scalar flux (Group 2) = 2.1363 n.cm^2/s

Table 2 Numerical results for the two-group heterogeneous benchmark problem with S_{16} quadrature

Method	*Mesh*	*x = 20*	*x = 56*	*x = 80*	δ_g	*CPU (s)*
ELD	32M[a]	3.3045e+00[b] 2.1325e+00[c]	1.7465e-07 1.2770e-07	2.5422e-14 3.2227e-14	4.5199e-04 7.5354e-04	3.7793e+01
	M	3.3047e+00 2.1208e+00	1.7448e-07 1.2807e-07	2.5854e-14 2.9459e-14	3.7161e-02 2.6064e-01	1.2535e+00
DD	32M	3.3044e+00 2.1325e+00	1.7385e-07 1.2712e-07	2.5074e-14 3.1787e-14	1.5955e-02 1.5955e-02	2.9109e+01
	M	3.2807e+00 2.1268e+00	–1.6963e-02 –6.5326e-03	–8.5483e-03 –1.7157e-03	2.7646e+15 1.0519e+15	5.5592e-01
LD	32M	3.3045e+00 2.1325e+00	1.7463e-07 1.2769e-07	2.5415e-14 3.2219e-14	3.4559e-04 5.4499e-04	3.9728e+01
	M	3.3137e+00 2.1077e+00	3.3028e-08 2.3492e-08	6.0746e-16 -3.7812e-15	1.0314e+00 1.1173e+00	1.4208e+00
SGF	32M	3.3044e+00 2.1325e+00	1.7465e-07 1.2770e-07	2.5422e-14 3.2227e-14	Ref.	6.6991e+02
	M	3.3044e+00 2.1325e+00	1.7465e-07 1.2770e-07	2.5422e-14 3.2227e-14	1.6319e-08 1.7585e-08	6.4298e+00

Note: [a]M = 5×9×6×5 cells,
[b]Scalar flux (Group 1) = 3.3045 n.cm^2/s,
[c]Scalar flux (Group 2) = 2.1325 n.cm^2/s

In Tables 1 and 2, some negative neutron flux values appear for DD and LD methods. The numerical results for these methods heavily depend on the spatial mesh. In coarse-mesh calculations, DD and LD methods can become unstable, and because of this instability, they produce non-physical solutions, like negative values. A detailed explanation of the S_N equations numerical schemes' instability is offered in (Larsen, 1986).

Figures 4(a) and 4(b) offer the neutron distribution along the problem domain for the S_2 and S_{16} quadratures. The neutron flux behaviour is consistent with the problem conditions. On the left-region $(0 \le x \le 20)$ where we have the neutron source and reflexive boundary condition at $x = 0$, the fast and thermal fluxes show a smooth-flat behaviour. After the interface $(x = 20)$, begins the non-source region and the neutron fluxes decrease abruptly first, and later, gradually decrease until the domain's right boundary. As the flux range, between left and right domain boundaries, is [1E1, 1E-19], we need to plot Figures 4(a) and 4(b) in logarithmic scale, to clarify the flux behaviour and the accuracy differences between numerical methods Figures 4(c) and 4(d). In these graphs, we can note that the DD and LD numerical results move away from the reference solution when the neutron fluxes decrease. In S_2 quadrature the ELD numerical solution reproduces the reference while in S_{16} quadrature is close. Owing the aforementioned elements, the ELD method is more accurate than DD and LD in coarse mesh calculations. In addition, the ELD method is more accurate in lower order quadrature because when N increases, the number of non-preserved eigenvalues $(G \times N - 2)$ also increases becoming the ELD approximation rougher.

Figure 4 Fast (blue) and thermal (red) neutrons distribution generated by the DD, LD, ELD and SGF methods for the heterogeneous benchmark problem. (a) S_2 quadrature with a linear scale, (b) S_{16} quadrature with a linear scale, (c) S_2 quadrature with a logarithmic scale and (d) S_{16} quadrature with a logarithmic scale

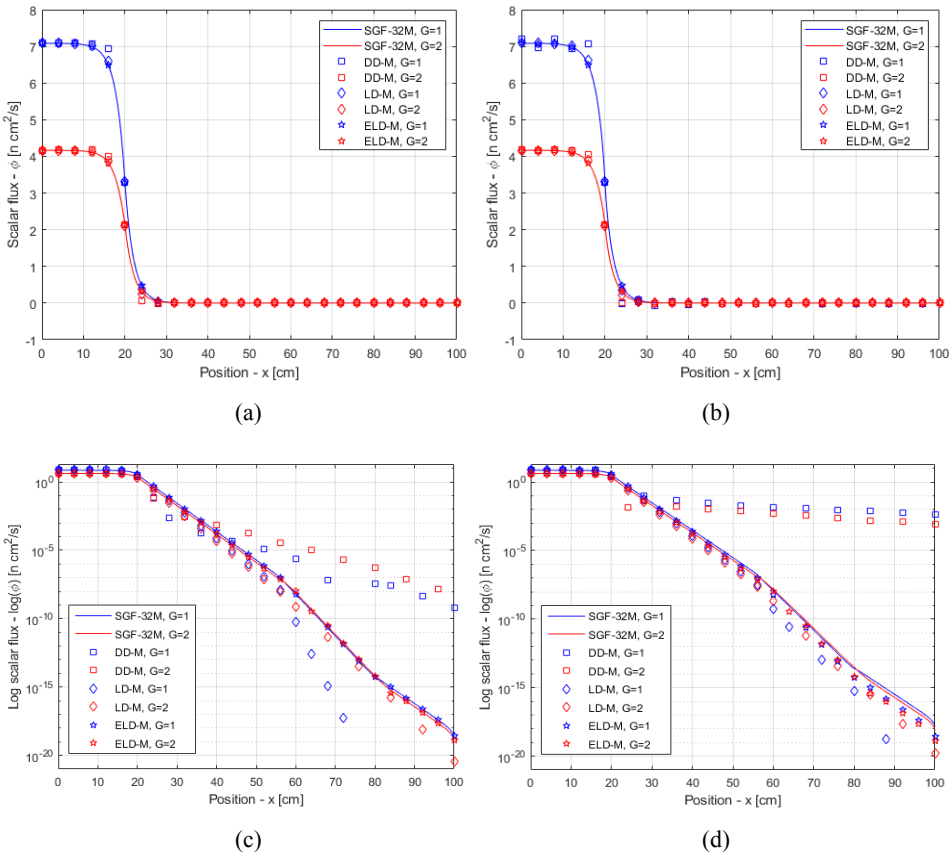

Figures 5 and 6 also offer the CPU time and relative deviations for the first benchmark problem considering different spatial meshes. The computational cost, evaluated in CPU times, increases for the highest quadrature order because we have more neutron travel directions in the balance equations. To achieve accurate numerical results (a relative deviation less than 5%), in S_2 quadrature, the DD, LD and ELD methods need respectively 48.91 (32M cells), 14.45 (8M cells) and 3.50 (M cells) times the CPU time reported by SGF method. On the other hand, for S_{16} quadrature the DD, LD and ELD methods require respectively, 4.53 (32M cells), 1.60 (8M cells) and 0.37 (M cells) times the CPU time registered by the SGF. In all cases, the ELD method reports better computational performance than the DD and LD methods, and also, for the SGF in S_{16} quadrature, considering the same spatial grid. We remark that the SGF method is spatial truncation errors free and the generated numerical results are mesh independent. For that reason, the SGF offers accurate results using one spatial cell per region. On the other hand, the ELD method is not spatial truncation errors free and the numerical results have a weak dependency on the spatial grid. Thus, the SGF method is more efficient computationally than the proposed ELD method.

Figure 5 Relative deviation and computational cost evaluated in CPU time, for heterogeneous problem and S_2 quadrature

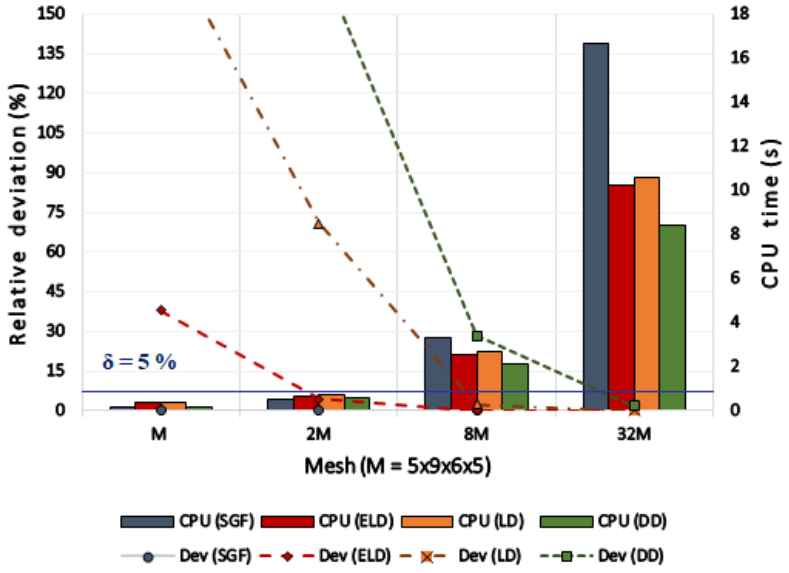

Our second model problem, reported by Garcia and Siewert (1981), consists of an iron homogeneous slab of 10 cm. Here, we consider a 19-energy group model distributed between 50 keV and 1 MeV. Unitary isotropic flow inlet related to the first group is prescribed on the domain left boundary and vacuum conditions are imposed on the right boundary.

Figure 6 Relative deviation and computational cost evaluated in CPU time, for heterogeneous problem and S_{16} quadrature

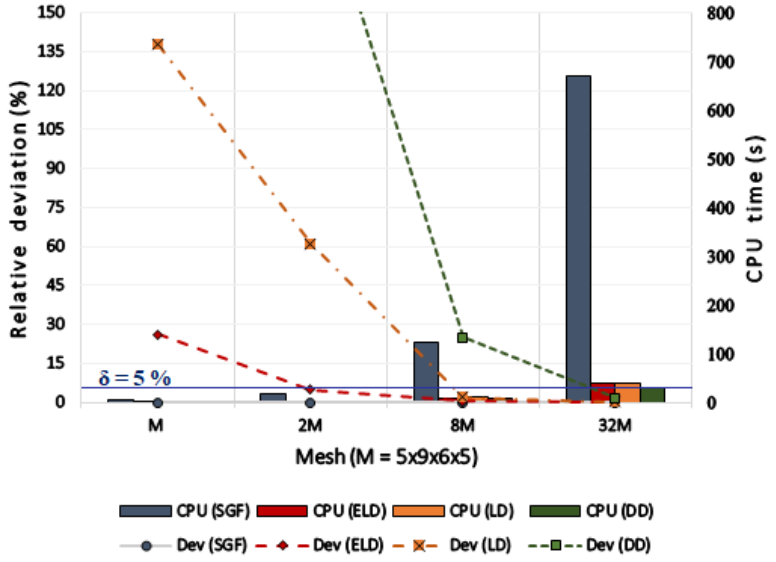

Tables 3 show the scalar flux generated by ELD, DD, LD and SGF methods at x = 0, 5 and 10 cm for the 1st, 10th and 19th group of energy in S_2 quadrature. For S_{16} quadratures this information appears in Table 4. The numerical results generated by the SGF method for the fine mesh (1600 cells) are used as reference solution.

As before, Tables 3 and 4 show that the numerical results generated by the ELD, DD and LD methods converge to the reference solution when the spatial cell size decrease. Also, the proposed method is still more accurate if compared to the DD and LD methods for the coarse mesh studied (100 cells), even, in less diffusive problems where angular flux gradients are stronger. Nevertheless, the mesh must become finer in order to achieve similar accurate results in comparison to the first benchmark problem. Also, we can notice that the numerical results generated by ELD method are more mesh dependent than the first problem. This is, due to that non-preserved eigenvalues number has more weight in the total kernel size. However, we notice an improvement in the results relative deviation for each energy group if compared with the DD and LD methods for S_2 and S_{16} quadratures. So, the proposed method relative deviation for each group is spectral dependent. Analysing Tables 1–4, is possible to observe that the ELD method accuracy is better when we use less energy-groups or few angular directions.

Table 3 Numerical results for the benchmark 19-groups, homogeneous problem with S_2 quadrature

Method	*Mesh*	*x = 0*	*x = 5*	*x = 10*	δ_g	*CPU (s)*
ELD	1600	5.0795e-01[a]	1.1545e-21	2.5823e-42	4.4669e-14	1.4476e+01
		1.3885e-02[b]	3.0376e-21	5.8540e-42	6.3514e-06	
		3.9759e-06[c]	5.8253e-24	3.0207e-45	2.2061e-03	
	100	5.0795e-01	1.1545e-21	2.5823e-42	2.8995e-14	9.0391e-01
		1.4064e-02	3.0584e-21	5.8618e-42	2.0787e-02	
		5.7613e-06	5.8692e-24	3.7060e-45	4.5139e-01	
DD	1600	5.0795e-01	1.1385e-21	2.5111e-42	2.7595e-02	1.1564e+01
		1.3885e-02	2.9963e-21	5.6927e-42	2.7545e-02	
		3.9695e-06	5.7461e-24	2.9332e-45	2.7544e-02	
	100	5.0795e-01	1.8011e-23	6.2849e-46	9.9976e-01	6.8860e-01
		1.3885e-02	5.0756e-23	1.4376e-45	9.9975e-01	
		3.9695e-06	–1.0150e-10	–9.5954e-15	3.1812e+30	
LD	1600	5.0795e-01	1.1543e-21	2.5816e-42	2.7278e-04	1.5464e+01
		1.3885e-02	3.0372e-21	5.8524e-42	2.7347e-04	
		3.9758e-06	5.8242e-24	3.0198e-45	2.1668e-03	
	100	5.0788e-01	7.1716e-22	9.9672e-43	6.1402e-01	9.6085e-01
		1.3916e-02	1.9000e-21	2.2572e-42	6.1441e-01	
		5.5820e-06	3.4937e-24	1.3828e-45	6.2442e-01	
SGF	1600	5.0795e-01	1.1545e-21	2.5823e-42		1.6255e+02
		1.3885e-02	3.0376e-21	5.8540e-42	Ref.	
		3.9695e-06	5.8253e-24	3.0163e-45		
	100	5.0795e-01	1.1545e-21	2.5823e-42	3.2944e-13	8.3533e+00
		1.3885e-02	3.0376e-21	5.8540e-42	8.9475e-12	
		3.9695e-06	5.8253e-24	3.0163e-45	1.8296e-06	

Note: [a]Scalar flux (Group 1) = 5.0795×10^{-1} n.cm^2/s,
[b]Scalar flux (Group 10) = 1.3385×10^{-2} n.cm^2/s,
[c]Scalar flux (Group 19) = 3.9759×10^{-6} n.cm^2/s

Table 4 Numerical results for the benchmark 19-groups, homogeneous problem with S_{16} quadrature

Method	*Mesh*	*x = 0*	*x = 5*	*x = 10*	δ_g	*CPU (s)*
ELD	1600	5.0795e-01[a]	1.0504e-14	2.7727e-27	6.0983e-05	4.3481e+01
		1.3391e-02[b]	3.6183e-15	5.4072e-28	2.0486e-04	
		4.1934e-06[c]	6.0793e-18	2.5348e-31	9.5456e-03	
	100	5.0773e-01	1.0471e-14	2.7679e-27	7.1714e-02	1.0883e+01
		1.3508e-02	3.6042e-15	5.4201e-28	4.0164e-02	
		6.4377e-06	6.0511e-18	3.2876e-31	5.4604e-01	
DD	1600	5.0795e-01	1.0470e-14	2.7555e-27	6.1934e-03	3.3872e+01
		1.3390e-02	3.6065e-15	5.3735e-28	6.2218e-03	
		4.1640e-06	6.0593e-18	2.5016e-31	4.9891e-02	
	100	5.0795e-01	4.4352e-15	5.2152e-28	8.1191e-01	2.0637e+00
		1.3390e-02	–2.6125e-12	–2.5695e-21	4.7520e+06	
		4.1640e-06	–1.0889e-07	–2.3467e-08	9.3228e+22	
LD	1600	5.0795e-01	1.0504e-14	2.7726e-27	6.1941e-05	4.6914e+01
		1.3390e-02	3.6183e-15	5.4070e-28	2.0202e-04	
		4.1934e-06	6.0790e-18	2.5347e-31	9.5206e-03	
	100	5.0767e-01	9.7785e-15	2.4238e-27	1.2584e-01	2.9247e+00
		1.3405e-02	3.3495e-15	4.7399e-28	1.2812e-01	
		6.3504e-06	5.5417e-18	2.8444e-31	5.2507e-01	
SGF	1600	5.0795e-01	1.0504e-14	2.7727e-27	Ref.	9.4383e+03
		1.3390e-02	3.6183e-15	5.4071e-28		
		4.1640e-06	6.0793e-18	2.5172e-31		
	100	5.0795e-01	1.0504e-14	2.7727e-27	2.2594e-14	4.6675e+02
		1.3390e-02	3.6183e-15	5.4071e-28	1.2273e-10	
		4.1640e-06	6.0792e-18	2.5169e-31	1.0525e-04	

Note: [a]Scalar flux (Group 1) = 5.0795×10^{-1} n.cm^2/s,
[b]Scalar flux (Group 10) = 1.3390×10^{-2} n.cm^2/s,
[c]Scalar flux (Group 19) = 4.1934×10^{-6} n.cm^2/s

Finally, high energy group problems involve much more computational cost in comparison to the first problem, and the ELD method relative speedup to obtain accurate numerical results (a relative deviation less than 5 %) is significant in relation to the other methods for the same spatial grid.

5 Conclusions and recommendations

In this work was present the mathematical formulation of the ELD method to solve one-dimensional fixed-source transport problems in multi-group discrete ordinates formulation. The proposed method is characterised by a weak spatial dependence in the generated solutions due to the auxiliary equations involved. These equations partially preserve the spectrum of the analytic S_N equations. We also present the iterative sweeping scheme used by the new method. This scheme, based on the source iteration approach, is simpler and requires fewer arithmetic operations per iteration if compared to the SGF method. The main advantages of the proposed method are that the numerical scheme is stable and its results weakly depend on the spatial cell dimension. In addition, the ELD method is more accurate than the DD and LD methods in coarse-mesh

calculations. Thus, we can conclude that the ELD method, based on a simpler sweep scheme, offers satisfactory numerical solutions for coarse-meshes with reasonable computational cost.

The ELD method preserves two eigenvalues of the analytic S_N equations spectrum. The spectrum size is $N \times G$, then $N \times G - 2$ is the non-preserve eigenvalues number. When the number of angular directions (N) or the energy groups (G) increases, the preserved eigenvalues number remains constant, meanwhile, the non-preserve eigenvalues number grows. In this situation, the approximation of ELD method becomes rougher. For that reason, more accurate results are obtained when we have few angular directions and a low number of energy groups.

We remark that we can improve the numerical results accuracy, preserving more than two eigenvalues in the auxiliary equations. Therefore, we propose the extension of this approach for Cubic Discontinuous (CD) and fifth-degree Discontinuous (5D) methods, and then verify its performance comparing them with the ELD method results. The CD and 5D methods will be able to preserve four and six kernel elements, respectively. Also, we suggest for future research the extension of this new method for multi-dimensional transport problems and to consider, anisotropic scattering source.

Another future development is to extend the ELD method for solving multiplicative problems. This extension is simple and intuitive. We can use a similar discretisation process to obtain the corresponding spatial balance equations and consider the same auxiliary equations, equation (11), to generate the iterative numerical scheme. Specifically, in criticality problems, the spectral parameters depend on the effective multiplication factor and must be updated in the iterative process. The advantages and disadvantages of ELD method must be the same for this kind of problems.

References

Abreu, M.P., Filho, H.A. and Barros, R.C. (1996) 'A numerical method for multigroup slab-geometry eigenvalue problems in transport theory with no spatial truncation error', *Transport Theory and Statistical Physics*, Vol. 25, No. 1, pp.61–83.

Alcouffe, R.E., Larsen, E.W., Miller, W.F. and Wienke, B.R. (1979) 'Computational efficiency of numerical methods for the multigroup, discrete-ordinates neutron transport equations: the slab geometry case', *Nuclear Science and Engineering*, Vol.71, pp.111–127.

Anli, F. and Gungor, S. (1996) 'A spectral nodal method for one-group X, Y, Z-Cartesian geometry discrete ordinates problems', *Annals of Nuclear Energy*, Vol. 23, No. 8, pp.669–680.

Barros, R.C. and Larsen, E.W. (1990) 'A numerical method for one-group slab-geometry discrete ordinates problems with no spatial truncation error', *Nuclear Science and Engineering*, Vol. 104, pp.199–208.

Barros, R.C. and Larsen, E.W. (1991) 'A numerical method for multigroup slab-geometry discrete ordinates problems with no spatial truncation error', *Transport Theory and Statistical Physics*, Vol. 20, pp.441–462.

Barros, R.C. and Larsen, E.W. (1992) 'A Spectral nodal method for one-group X, Y-geometry discrete ordinates problems' *Nuclear Science and Engineering*, Vol. 111, pp.34–45.

Barros, R.C. (1997) 'On the equivalence of discontinuous finite element methods and discrete ordinates methods for the angular discretization of the linearized Boltzmann equation in slab geometry', *Annals of Nuclear Energy*, Vol. 24, No. 13, pp.1013–1026.

Barros, R.C., Yavuz, M., Abreu, M.P., Filho, H.A. and Mello, J.A.M. (1998) 'Progress in spectral nodal methods applied to discrete ordinates transport problems', *Progress in Nuclear Energy*, Vol. 33, pp.117–154.

Barros, R.C., Silva, F.C. and Filho, H.A. (1999) 'Recent advances in spectral nodal methods for X, Y-geometry discrete ordinates deep penetration and eigenvalue problems', *Progress in Nuclear Energy*, Vol. 35, pp.293–331.

Barros, R.C., Filho, H.A., Orellana, E.T.V., Silva, F.C., Couto, N., Dominguez, D.S. and Hernández, C.R. (2003) 'The application of spectral nodal methods to discrete ordinates and diffusion problems in Cartesian geometry for neutron multiplying systems', *Progress in Nuclear Energy*, Vol. 42, pp.385–426.

Barros, R.C., Filho, H.A., Platt, G.M., Oliveira, F.B. and Militao, D.S. (2010) 'Analytical reconstruction scheme for the coarse-mesh solution generated by the spectral nodal method for neutral particle discrete ordinates transport model in slab geometry', *Annals of Nuclear Energy*, Vol. 37, pp.1461–1466.

Dominguez, D.S. and Barros, R.C. (2007) 'The spectral Green's function linear-nodal method for one-speed X, Y-geometry discrete ordinates deep penetration problems', *Annals of Nuclear Energy*, Vol. 34, pp.958–966.

Dominguez, D.S., Oliveira, F.B.S., Filho, H.A. and Barros, R.C. (2010) 'Composite spatial grid spectral nodal method for one-speed discrete ordinates deep penetration problems in X, Y geometry', *Progress in Nuclear Energy*, Vol. 52, pp.298–303.

Dominguez, D.S., Rocha, R.V.M., Iglesias, S.M., Escrivá, A. and Filho, H.A. (2018) 'A composite spatial grid spectral Green's function method for one-speed discrete ordinates eigenvalue problems in two-dimensional Cartesian geometry', *Progress in Nuclear Energy*, Vol. 109, pp.180–187.

Filho, H.A., Silva, F.C. and Barros, R.C. (2002) 'A coarse-mesh numerical method for one-speed neutron transport eigenvalue problems in two-dimensional Cartesian geometry', *Applied Numerical Mathematics*, Vol. 40, pp.167–177.

Garcia, R.D.M. and Siewert, C.E. (1981) 'Multigroup transport theory. II. Numerical Results', *Nuclear Science and Engineering*, Vol. 78, pp.315–323.

Hill, T.R. (1975) *ONETRAN: A Discrete Ordinates Finite Element Code for the Solution of the One-Dimensional Multigroup Transport Equation*, Los Alamos National Laboratory, Technical report LA-5990-MS.

Larsen, E.W. (1986) 'Spectral analysis of numerical methods for discrete-ordinates problems I', *Transport Theory and Statistical Physics*, Vol. 15, pp.93–116.

Lewis, E.E. and Miller, J.W.F. (1984) *Computational Methods of Neutron Transport*, 1st ed., John Wiley & Sons, New York.

Mello, J.A.M. and Barros, R.C. (2002) 'An exponential spectral nodal method for one-group X, Y-geometry deep penetration discrete ordinates problems', *Annals of Nuclear Energy*, Vol. 29, pp.1855–1869.

Menezes, W.A., Filho, H.A. and Barros, R.C. (2014) 'Spectral Green's function nodal method for multigroup S_N problems with anisotropic scattering in slab-geometry non-multiplying media', *Annals of Nuclear Energy*, Vol. 64, pp.270–275.

Silva, D.J.M., Filho, H.A. and Barros, R.C. (2015) 'A spectral nodal method for eigenvalue S_N transport problems in two-dimensional rectangular geometry for energy multigroup nuclear reactor global calculations', *Proceedings of the International Nuclear Atlantic Conference*, Belo Horizonte, Brazil.

Rivas-Ortiz, I.B., Sanchez-Dominguez, D., García-Hernández, C.R., Iglesias, S.M. and Escrivá, A. (2019) 'An extended linear discontinuous method for one-group fixed source discrete ordinates problems with isotropic scattering in slab geometry', *Tendências em Matemática Aplicada e Computacional*, Vol. 29, No. 1.

Rocha, R.V.M., Dominguez, D.S., Iglesias, S.M. and Barros, R.C. (2016) 'Finite element method with spectral green's function in slab geometry for neutron diffusion in multiplying media and one energy group', *Tendências em Matemática Aplicada e Computacional*, Vol. 17, No. 2, pp.173–185.